

# Dynamic Heterogeneity in Poly(vinyl methyl ether)/Poly(2-chlorostyrene) Blends

C. M. Roland,<sup>\*,†</sup> K. J. McGrath,<sup>†,‡</sup> and R. Casalini<sup>†,‡</sup>

Chemistry Division, Naval Research Laboratory, Code 6120, Washington DC 20375-5342, and  
Chemistry Department, George Mason University, Fairfax, Virginia 22030

Received February 10, 2006; Revised Manuscript Received March 24, 2006

**ABSTRACT:** Dielectric spectroscopy was used to follow the component dynamics in the miscible blend of poly(vinyl methyl ether) (PVME) and poly(2-chlorostyrene) (P2CS). For the PVME component (which has the more intense loss peak due to its higher polarity), the shape of the segmental relaxation peak depends only on the relaxation time and is otherwise independent of thermodynamic conditions. This is in accord with the general behavior of neat materials. By measuring the spectra as a function of both temperature and pressure, the relative effect of temperature and volume on the segmental relaxation times was quantified from ratio of the isochoric and isobaric activation enthalpies. This ratio is essentially the same for the neat polymers, but blending has a disparate effect of the components: volume effects become stronger for the PVME but are diminished for P2CS. Similarly, the fragilities of the neat components are quite close but change markedly in the blend. The P2CS component has a fragility of 32, which is lower than found for any neat polymer. In comparison to the segmental dynamics, transport of mobile ions in the blend is relatively insensitive to volume (or pressure). These effects are reflected in the magnitude of the respective exponents of the scaling function, which enables collapse of the relaxation times onto single, component-specific master curves.

## Introduction

Polymer blends are interesting to study for many reasons, including their technological importance (allowing properties to be varied without synthesis of new materials) and the insights that can be gleaned into structure/property relationships. Of particular fundamental interest are miscible blends, and since molecular motions underlie their processability and many physical properties of polymers, most studies focus on the segmental dynamics of miscible blends. Relevant issues include the role of self-concentration effects due to polymer segment connectivity,<sup>1,2</sup> the intrinsic mobility differences among polymers and how that translates to the mixture,<sup>3–7</sup> and the cause of various anomalies observed in many blends under specific conditions.<sup>8–11</sup> Various theories of the dynamics of blends have been proposed;<sup>2,12–19</sup> however, given the status of the glass transition in neat materials as a major unsolved problem, theoretical efforts are likely to remain at the model-building stage for the foreseeable future.

Much progress has been made in understanding the relaxation properties of blends, in large measure due to the accumulation of much experimental data.<sup>17,19–28</sup> In this paper we compare the dielectric relaxation of poly(2-chlorostyrene) (P2CS) and poly(vinyl methyl ether) (PVME) to their behavior when blended. P2CS and PVME are thermodynamically miscible due to the interaction of the phenyl ring of the P2CS with the PVME methoxy group.<sup>29</sup> This interaction is enhanced by virtue of the electronegative halogen on the P2CS.<sup>30</sup> A miscible blend has a morphology that is homogeneous on the segmental level; each component experiences the same average environment apart from chain connectivity. However, the interaction of the components with their local environment, as well as intrinsic mobility differences, can cause them to exhibit different relaxation times (i.e., distinct component  $T_g$ 's), a phenomenon

referred to as dynamic heterogeneity.<sup>1,3,4,6,8,31,32</sup> In P2CS/PVME blends, dynamic heterogeneity was observed with dielectric spectroscopy by Urakawa et al.<sup>33</sup> and using thermally stimulated depolarization current measurements by Leroy et al.<sup>34</sup> Together with the fact that both components are polar, this dynamic heterogeneity means that the dynamics of each component can be monitored as a function of temperature and pressure.

Pressure is an important variable in studying the dynamics of neat materials, since it allows deconvolution of the effects of thermal energy and density.<sup>35</sup> There have been only a few studies of the effect of pressure on the dynamics of blends or block copolymers. Pressure weakens the H-bonding in blends of poly(vinylphenol) with poly(vinyl ethyl ether), causing a broadening of the dielectric relaxation peak.<sup>24</sup> In poly(isoprene-*b*-vinylethylene) diblock copolymer (PI-*b*-PVE), Floudas et al.<sup>26</sup> found that high pressure causes the relaxation spectrum to narrow; that is, under conditions of high  $P$  and  $T$  the degree of dynamic heterogeneity is reduced. The faster  $\alpha$ -relaxation of the (lower  $T_g$ ) PI block shifts to lower frequency, merging with the peak from the PVE. This was attributed to the greater pressure sensitivity (larger activation volume) of the (lower  $T_g$ ) PI segments.<sup>26</sup>

On the other hand, in dielectric studies of blends of polystyrene with poly(vinyl methyl ether) (PS/PVME),<sup>36,37</sup> elevated pressure had no effect beyond increasing the blend  $T_g$ . The segmental relaxation time distributions (measured for the PVME only, since the dipole moment of PS is too weak) were the same for different temperature–pressure conditions compared at a fixed value of the mean relaxation time. Note that for this blend the component with the larger activation volume (PS) also has the higher  $T_g$ .<sup>36,38,39</sup> If the relative magnitude of the activation volume for each component remains unchanged upon blending, the expectation is that pressure will move the lower frequency PS even further from the PVME peak.

Polymer blends are sometimes miscible due to the presence of hydrogen bonding between the components; moreover, this association of the components can make them more dynamically

<sup>†</sup> Naval Research Laboratory.

<sup>‡</sup> George Mason University.

homogeneous. Although temperature reduces the degree of hydrogen bonding, the effect of pressure is more complicated.<sup>40–46</sup> Since higher pressure measurements are usually carried out at higher temperatures, the general finding is that pressure reduces H-bonding. This is seen in blends of poly(4-vinylphenol) (PVPh) with poly(vinyl ethyl ether), which become more dynamically heterogeneous at increased pressure, due to a decrease in H-bonding between the components.<sup>24</sup> However, in blends of PVPh with poly(ethylene-*co*-vinyl acetate) (EVA),<sup>47</sup> the dielectric  $\alpha$ -relaxation peak becomes narrower at high pressure and temperature, implying more homogeneous dynamics. This is an unexpected result, since the higher  $T_g$  component (PVPh) has the larger activation volume.<sup>47</sup>

Thus, although there have been only a limited number of studies of blends, the effect of pressure on the dynamics has been found to vary markedly. Certainly more work is needed to clarify the factors that influence the effect pressure has on blend dynamics. The present investigation is the first in which high-pressure measurements are carried out on a dynamically heterogeneous blend; that is, one in which distinct component  $\alpha$ -relaxation peaks can be observed. Thus, we are able to follow the effect blending has on the dynamics of each component. This included comparing the relative influence of density and temperature on the relaxation times and assessing the applicability of the scaling of  $\alpha$ -relaxation times known for neat glass-formers.<sup>48,49</sup>

## Experimental Section

The poly(2-chlorostyrene) (P2CS) (weight-average molecular weight,  $M_w = 58$  kg/mol, polydispersity = 2.1) and poly(vinyl methyl ether) (PVME) ( $M_w = 99$  kg/mol, polydispersity = 2.1) were obtained from Scientific Polymer Products. The P2CS was used as received while the PVME was dried in vacuo for a week at  $T \sim 55$  °C and then kept in a drybox. The blend was prepared by dissolution in toluene, with subsequent drying for 1 day at ambient conditions, followed by 1 week at 60 °C in vacuo. For dielectric measurements the blend solution was cast directly onto the electrodes followed by drying; the neat P2CS was molded directly between two electrodes. For pressure–volume–temperature (PVT) measurements, samples were molded under vacuum into a cylinder. The ambient density was measured by the buoyancy method, and the temperature and pressure dependences of the specific volume were measured with a Gnomix instrument.<sup>50</sup> The temperature was scanned at 0.5 deg/min for the latter.

Dielectric spectra were obtained with a parallel plate geometry using an IMASS time domain dielectric analyzer ( $10^{-4}$ – $10^3$  Hz) and a Novocontrol Alpha analyzer ( $10^{-2}$ – $10^6$  Hz). For measurements at elevated pressure, the sample was contained in a Harwood Engineering pressure vessel, with hydraulic pressure applied using a Enerpac pump in combination with a pressure intensifier (Harwood Engineering). Pressures were measured with a Sensotec tensometric transducer (resolution = 150 kPa). The sample assembly was contained in a Tenney Jr. temperature chamber, with control to within  $\pm 0.1$  K at the sample. Atmospheric pressure measurements on the blend were carried out in a closed-cycle helium cryostat in a helium atmosphere, with control to within  $\pm 0.01$  K. For the neat P2CS, ambient pressure data were obtained with the sample in a Delta Design oven (temperature stability =  $\pm 0.1$  K) with a nitrogen atmosphere. The dielectric and PVT results herein for neat PVME were published previously.<sup>38</sup> Differential scanning calorimetry was carried out using a TA Instruments Q100 with liquid nitrogen cooling. Data were obtained during cooling from the liquid state through  $T_g$  at 10 K/min. The upper temperature for the blend ( $\sim 430$  K) was below the ambient pressure LCST.<sup>30</sup> Generally, pressure is expected to elevate the LCST,<sup>35,51</sup> and moreover no indications of phase separation were apparent herein in the dielectric spectra or the volumetric data.

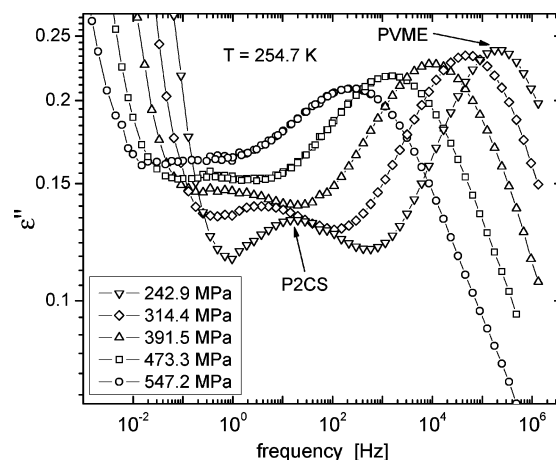


**Figure 1.** Representative dielectric loss spectra for the blend at various pressures and the indicated temperature.

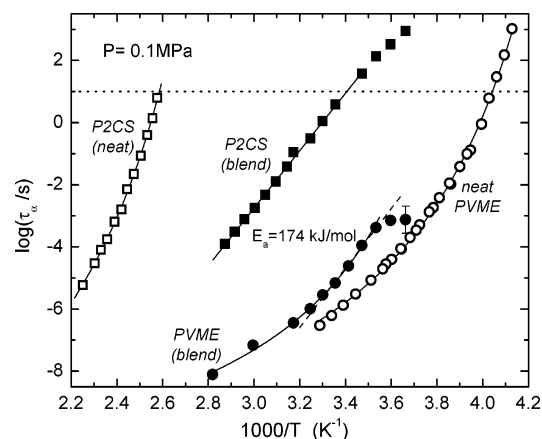


**Figure 2.** Relaxation times at ambient pressure for the neat components (hollow symbols) and the blends (filled symbols). For PVME component, data for  $\tau < 10^{-6}$  s were obtained by extrapolation of pressure dependences in Figure 4. The dashed line for PVME in the blend has the same slope as the  $\tau(T)$  data for P2CS in the blend, corresponding to the indicated value of the apparent activation energy. The dotted line denotes  $\tau_\alpha(T_g)$ . Note that in the blend, when  $\tau_\alpha$  for P2CS becomes long,  $\tau_\alpha$  for PVME becomes almost temperature invariant.

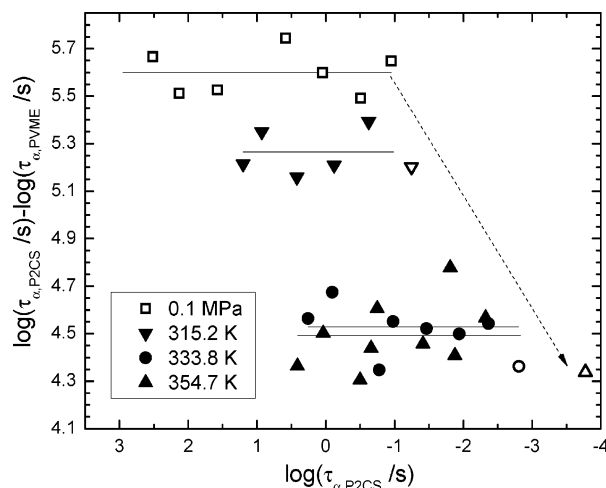
## Results

In Figure 1 are representative dielectric loss spectra obtained at fixed  $T = 254.7$  K and various pressures. The two distinct peaks in each spectrum, corresponding to structural relaxation of each component, are a manifestation of this blend's dynamic heterogeneity.<sup>3,33,34</sup> Additionally, toward lower frequencies there is a prominent contribution to the dielectric loss from dc conductivity,  $\epsilon''_{dc} \sim \sigma_{dc}/\omega$ , due to the presence of mobile ionic contaminants. Accounting for the conductivity, the partially overlapping peaks are simultaneously fit to two Havriliak–Negami functions,<sup>52</sup> with segmental relaxation times,  $\tau_\alpha$ , then defined as the inverse of the frequency of the maximum of the deconvoluted peak.

Arrhenius plots of the relaxation times measured at atmospheric pressure for the pure components are displayed in Figure 2.  $T_g$ 's defined at  $\tau_\alpha(T_g) = 10$  s differ by 140 deg (Table 1 has both the calorimetric  $T_g$ 's and the values determined from the dielectric measurements), so that the  $\alpha$ -relaxation times are separated by many orders of magnitude. The blend relaxation times for ambient pressure are included in Figure 2. The dispersions for the components are closer in frequency than for the neat polymers but still separated by more than 5 decades, enabling both peaks to be resolved. (Note that the spectra at

Table 1. Thermal and Relaxation Properties

	neat PVME	neat P2CS	PVME (blend)	P2CS (blend)	$\sigma_{dc}$ (blend)
$T_g$ (K) (DSC)	249.8	398.7	289.1		
$T_g$ (K) ( $\tau_\alpha = 10$ s)	247.3	386.7	<273 K	293.6 K	
$m$ ( $P = 0.1$ MPa)	80	72		32	
$\Delta V$ (mL/mol)	64 at 247.5 K		63–101 <sup>a</sup>	66–105 <sup>a</sup>	38–66 <sup>a</sup>
$\gamma$	2.55	2.6 $\pm$ 0.2	2.9	1.9	1.7

<sup>a</sup> 355 >  $T$  (K) > 315.

**Figure 3.** Difference in  $\alpha$ -relaxation times for blend components as temperature is varied at ambient pressure ( $\square$ ) and as pressure is varied at constant temperature. The pressure range is 38–147 MPa at 315.2 K, 42–267 MPa at 333.8 K, and 129–442 MPa at 354.7 K. The hollow symbols ( $\nabla$ ,  $\circ$ ,  $\triangle$ ) for the three isotherms represent extrapolations of the data in Figure 4 to 0.1 MPa. The dotted line is only to guide the eyes.

ambient pressure were measured at lower  $T$  than the elevated pressure measurements in order to have the peaks fall within the measurement range.)

The fragility, or steepness of  $T_g$ -normalized Arrhenius plots,  $m \equiv (d \log \tau_\alpha / (T_g dT^{-1}))$ , is a common measure of the temperature dependence of  $\tau_\alpha$ . The fragilities of the two neat components are close ( $= 72$  and  $80$  for P2CS and PVME, respectively), while in the blend  $m$  of P2CS is reduced to a value of only 32. For PVME in the blend the relaxation times cannot be measured at sufficiently low values for determination of the fragility; however, both blend curves in Figure 2 have nearly equivalent slopes above  $T_g$ , corresponding to an apparent activation energy,  $E_a = 174 \pm 5$  kJ/mol.

At fixed temperature, it can be seen in Figure 3 that the separation of the respective component  $\alpha$ -peaks is virtually independent of pressure, reflecting comparable pressure dependences. This pressure variation is quantified using the activation volume,  $\Delta V \equiv \ln(10)RT[(d \log \tau_\alpha)/dP]_T$ , which is a constant for low pressure. Results for the blend are shown in Figure 4, with the resulting  $\Delta V$  listed in Table 1.  $\Delta V$  increases inversely with temperature, and at each temperature the activation volume is essentially equivalent for the two components. It is larger (at comparable  $\tau_\alpha$ ) than the activation volume reported for neat PVME,  $\Delta V = 64$  mL/mol at  $T_g = 247.5$  K.<sup>38</sup>

Interestingly, the strength of the PVME relaxation decreases with increasing pressure,  $\Delta\epsilon/dP = -2.6$  GPa<sup>-1</sup> ( $\pm 0.7$ ) (Figure 5). Since the dipole density increases with  $P$ , this reduction in dielectric strength evidently reflects a loss of local correlation, presumably resulting from the presence of the P2CS segments. Neat PVME exhibits the more usual behavior, the dielectric strength increasing with pressure,  $\Delta\epsilon/dP = 0.1$  GPa<sup>-1</sup>.<sup>38</sup> Similarly, for P2CS in the blend,  $\Delta\epsilon/dP$  is positive, equal to

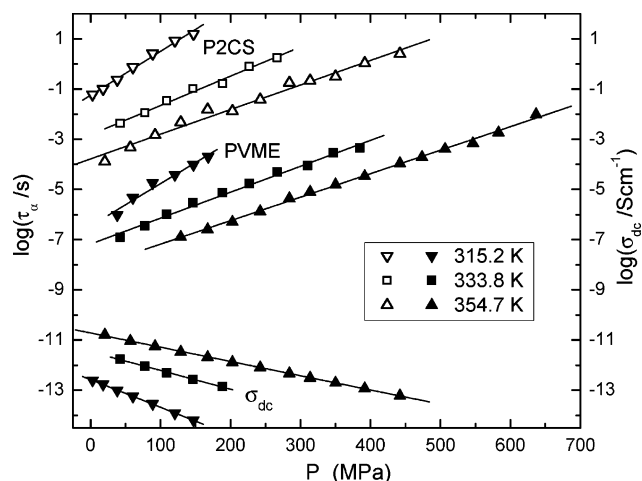


**Figure 4.** Pressure variation of the relaxation times for blend components (upper curves), along with dc conductivity (lower curves) of the blend, at the indicated temperatures.

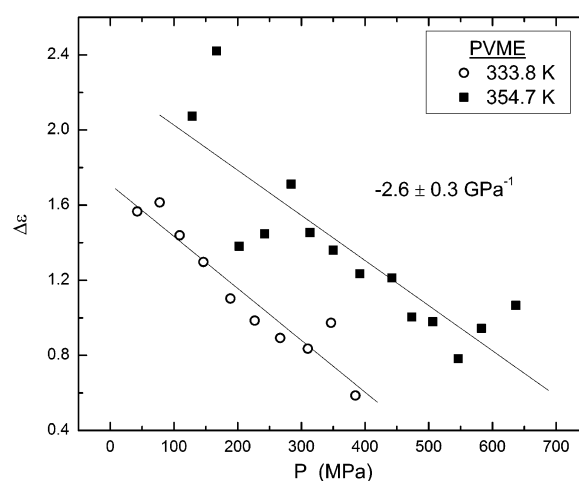


**Figure 5.** Dielectric strength of PVME in the blend as a function of pressure at the indicated temperatures.

about 3 GPa<sup>-1</sup> at 333.8 K. The consequence of these variations in dielectric strength of the blend components is a large change in the relative intensity of the two peaks with pressure. This is illustrated in Figure 6, showing the loss spectra for four conditions of  $T$  and  $P$ , all corresponding to a nearly constant value of  $\tau_\alpha$  for the PVME component. Although the P2CS peak is too weak for conclusions to be drawn, it is clear that the shape of the PVME peaks is constant at a fixed value of the segmental relaxation times, independently of the combination of temperature and pressure giving rise to the particular value of  $\tau_\alpha$ .

To analyze the blend dynamics further, we calculate the volume dependence of the relaxation times, using the  $T$  and  $P$  dependences in combination with the equation of state (EOS). The Tait equation<sup>53</sup> is fit to  $PVT$  data measured above  $T_g$

$$V(T, P) = (a_0 + a_1 T + a_2 T^2) [1 - 0.0894 \ln(1 + P/b_0 \exp(-b_1 T))] \quad (1)$$

where  $V$  is the specific volume. The respective parameters  $a_0$ ,  $a_1$ ,  $a_2$ ,  $b_0$ , and  $b_1$  for the neat polymers and the blend are listed in Table 2 (results for neat PVME taken from ref 38).

The relaxation times for both blend components are plotted in Figure 7 vs  $V$ . The isotherms all exhibit different behavior, clearly indicating that volume does not uniquely govern the

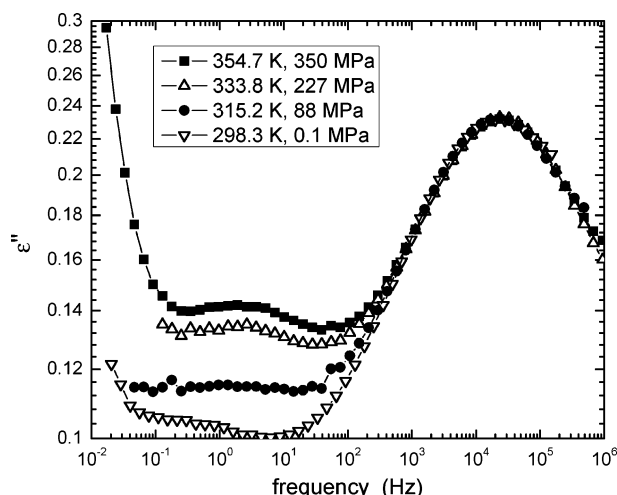


**Figure 6.** Comparison of loss spectra for the blend at combinations of  $T$  and  $P$  such that  $\tau_\alpha$  for the PVME is essentially constant. To superpose the peaks, the frequencies for  $P = 0.1$  and 227 MPa have been multiplied by 1.2 and 1.4, respectively, while the ordinate values for  $P = 88$  and 227 MPa have been multiplied by 1.33 and 1.3, respectively.

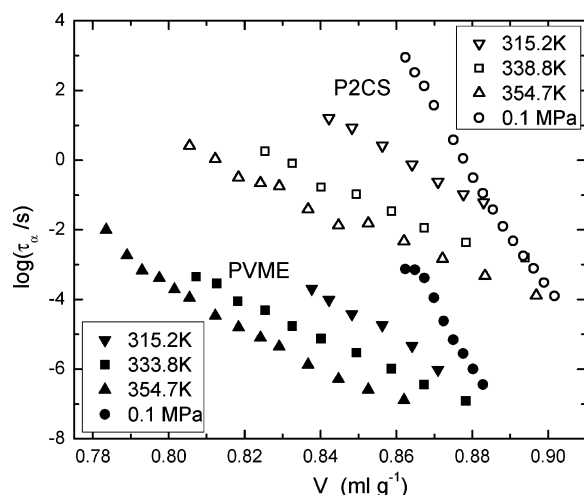


**Figure 7.** Volume dependence of the relaxation times for the blend components (from data in Figures 2 and 4).

**Table 2.** Tait EOS Parameters

	$a_1$ (mL/g)	$a_2$ (mL/(g C))	$a_3$ (mL/(g C <sup>2</sup> ))	$b_0$ (MPa)	$b_1$ (C <sup>-1</sup> )
neat PVME	0.9564	$5.587 \times 10^{-4}$	$4.256 \times 10^{-7}$	236.0	$4.745 \times 10^{-3}$
50/50 blend	0.8625	$4.971 \times 10^{-4}$	$3.580 \times 10^{-7}$	247.0	$3.787 \times 10^{-3}$
neat P2CS	0.7792	$3.000 \times 10^{-4}$	$5.510 \times 10^{-7}$	334.3	$5.02 \times 10^{-3}$

dynamics. The steeper slope of the isobaric ( $P = 0.1$  MPa) data reflects the additional effect of thermal energy on  $\tau_\alpha(T)$ . To quantify the relative  $V$  and  $T$  dependences of  $\tau_\alpha$ , we superpose the latter by plotting vs  $TV^\gamma$ , where the exponent  $\gamma$  is a constant determined empirically for each component. The obtained master curves of  $\tau_\alpha(TV^\gamma)$  are shown in Figure 8. Included is the conductivity data, for which  $\gamma = 1.7$  brings the isotherm and isobars into coincidence.

Although the dc conduction is due to ionic impurities, it is related to the mobility of the host. This is expressed by the empirical relation<sup>54</sup>

$$\sigma_{dc}\tau_\alpha^s = \text{constant} \quad (2)$$

where  $s \leq 1$ . The Debye–Stokes–Einstein equation, based on proportionality of the viscosity to relaxation times and inverse

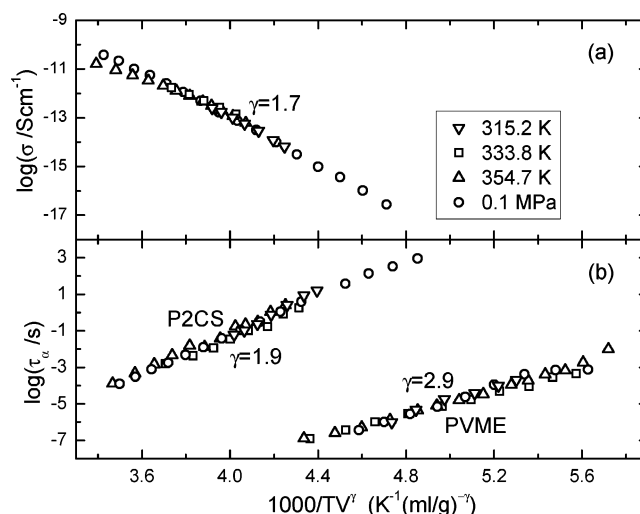


**Figure 8.** (a) Conductivity and (b) relaxation times plotted vs the inverse product of temperature times specific volume with the latter raised to the power of  $\gamma = 1.7$  ( $\sigma_{dc}$ ), 1.9 ( $\tau_\alpha$ , P2CS), and 2.9 ( $\tau_\alpha$ , PVME). Isobaric data at  $P = 0.1$  MPa (○); isotherms at  $T = 315.2$  K (▽), 333.8 K (□), and 354.7 K (△).

diffusion constants, corresponds to a value of unity for the exponent, while the enhancement of translational motions expected in the supercooled regime leads to  $s < 1$ .<sup>55–57</sup> At fixed temperature, the two components exhibit equivalent values of the exponent,  $s \sim 0.64$ , reflecting significant decoupling of translations and reorientational motions. For measurements at constant pressure,  $s$  for PVME is somewhat larger (Figure 9). Another manifestation of the decoupling phenomenon is the weaker pressure sensitivity of the conductivity in comparison to that of  $\tau_\alpha$ ,  $\Delta V$  being about  $1/3$  smaller for  $\sigma_{dc}$  than for  $\tau_\alpha$  (Figure 4 and Table 1).

## Discussion and Summary

**Dynamic Heterogeneity.** The blend of P2CS/PVME is of particular interest because of its substantial dynamic heterogeneity, a consequence of the large difference ( $\sim 140$  deg) in the neat component  $T_g$ 's. This gives rise to distinct  $\alpha$ -peaks in the dielectric loss spectra, enabling the motions of both components to be analyzed. For the PVME component, which can be more accurately resolved, the loss peaks superpose when measured at various combinations of  $T$  and  $P$  corresponding to a fixed peak frequency (Figure 6). This is in accord with a general experimental result for neat materials: for a given glass-forming material at a fixed value of  $\tau_\alpha$ , the dispersion is invariant to thermodynamic conditions; that is, the shape of the relaxation function depends solely on the relaxation time.<sup>58,59</sup> There is an additional factor in blends, concentration fluctuations, that can lead to departures from this empirical  $T$ – $P$  superpositioning. Concentration fluctuations govern the distribution of local environments, and these may change with  $T$  and  $P$  such that the shape of the loss peak may change. A priori, there is no reason that the distribution of local environments in a blend will conform to any  $T$ – $P$  superpositioning; nevertheless, equivalence of the segmental relaxation peaks at fixed  $\tau_\alpha$  is observed herein. It was also reported for PVME blended with PS by Alegría et al.,<sup>36</sup> although that situation is different because the dielectric loss for only one of the components was observed (the contribution from the weakly polar PS being too small). Accordingly, the absence of any change in peak shape has no bearing on dynamic heterogeneity per se but only reflects the invariance of the PVME dynamics at fixed  $\tau$ . Similarly, the results of Floudas et al.<sup>26</sup> on PI-*b*-PVE block copolymers, which



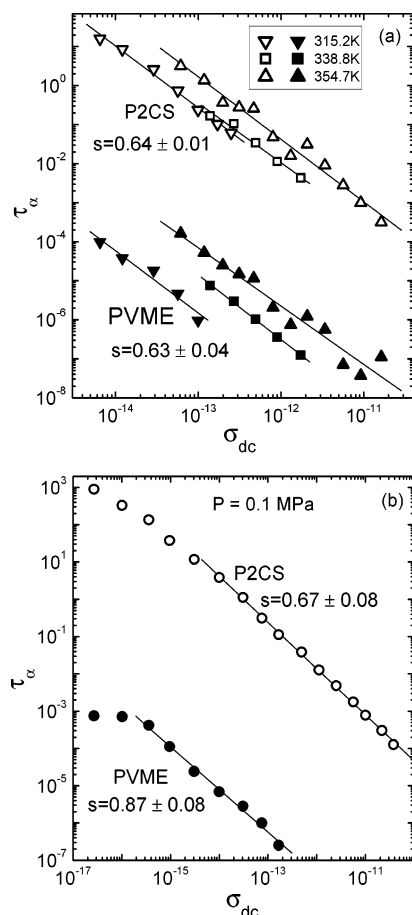


**Figure 9.** Decoupling of the ionic conductivity from the segmental relaxation, as indicated by  $s$  (eq 2) less than unity for (a) isothermal measurements and (b) isobaric data for the liquid state.

indicate a narrowing of the dielectric loss peak with pressure, say nothing about the relative separation of the component dispersions, since the distinct peaks cannot be distinguished and a change in shape or intensity of each peak would have the same effect.

The situation for P2CS/PVME is different, since the  $\alpha$ -dispersion for both components can be observed. This allows direct determination of the effect of pressure on the dynamic heterogeneity. We find (Figure 3) that for increasing pressure at fixed  $\tau$  the peaks become closer, while at fixed  $T$  their separation is essentially unchanged with  $P$ . The isotherms in Figure 3 could not be measured at  $P = 0.1$  MPa due to temperature limitations of the equipment. However, at sufficiently high temperatures these curves must coincide with the atmospheric pressure isobaric data. This extrapolated behavior is indicated by the dashed line in Figure 3. Also, note that at very high  $T$  the two components must have the same relaxation time (tending to the “universal value” of  $\log(\tau_\alpha) \sim 14$ – $16$ <sup>60</sup>), so that the upper curve (open squares) in Figure 3 must approach a value of zero in the high  $T$  limit (i.e., small  $\tau_\alpha$ ).

**Fragility.** Although the neat components have very different  $T_g$ 's, their intrinsic mobilities are otherwise quite similar; for example, at atmospheric pressure the fragilities differ by only  $\sim 10\%$  (Table 1). However, there is an enormous decrease in fragility for both components upon blending. At ambient pressure, the isobaric fragility of the P2CS is reduced by more than half to a value of 32, which is smaller than has been reported for any neat polymer.<sup>61</sup> Although  $m$  cannot be measured on the PVME in the blend (because its relaxation times are too short over the measurable range), the Arrhenius curves of  $\tau_\alpha$

for the two components are parallel (Figure 2), with slopes equating to a very small apparent activation energy,  $=174$  kJ/mol, consistent with the small  $m$ . Similarly, the ionic conductivity in the blend has a very weak temperature dependence,  $E_a \sim 150$  kJ/mol at atmospheric pressure.

When the P2CS component is in the glassy state ( $\tau_\alpha > 100$  s in Figure 2), the dynamics of the PVME become almost insensitive to temperature, as seen in the leveling off of the data at the lowest temperatures in Figure 2. Thus, a weakly temperature-dependent  $\tau_\alpha$  becomes virtually constant. Lorthioir et al.<sup>62</sup> have measured PVME in blends with PS and observed a speeding up of the PVME when the concentration of the polystyrene is high. They ascribed this to a confinement effect—the mobile PVME segments are constrained by being confined within regions of glassy PS. Certainly the PVME dynamics herein are much faster (by as much as a factor of 5) than expected from extrapolation of  $\tau_\alpha$  measured at temperatures for which the P2CS is still in the liquid state.

**Volume Effects on  $\tau$ .** The superposition of relaxation times for one component of a polymer blend when  $\tau_\alpha$  is plotted as a function of  $TV^\gamma$  was shown previously.<sup>63</sup> However, in the present case we can not only verify that  $\tau_\alpha$  for both components conform to this scaling but also compare the value of the respective scaling exponents. We find that in the blend  $\gamma = 1.9$  and  $2.9$  for P2CS and PVME, respectively (Figure 8). The fact that  $\gamma$  differs for each component means that this parameter cannot be related to a macroscopic property (such as the EOS) but must be related to the local structure. The different  $\gamma$  reveals the different interaction of the P2CS and PVME segments with their surroundings, which on average are the same, apart from chain connectivity. Interestingly,  $\gamma$  for PVME in the blend herein is essentially the same as that determined for PVME in a blend with PS (having the same concentration).<sup>63</sup>

Not only are the fragilities of the neat components nearly equal, but their relaxation behaviors are governed to a similar degree by volume relative to the effect that temperature has on  $\tau_\alpha$ . This is seen in the equivalence of the scaling exponents,  $\gamma = 2.55$  for neat PVME<sup>38</sup> and  $= 2.6 \pm 0.2$  for neat P2CS. A more intuitive metric of the relative contribution of temperature and volume to the relaxation is the ratio of the apparent activation energy at constant volume,  $E_V(T,V) \equiv R((\partial \ln \tau)/\partial T^{-1})_V$  to the constant pressure activation enthalpy,  $E_P(T,P) \equiv R((\partial \ln \tau)/\partial T^{-1})_P$ .<sup>64,65</sup>  $E_V/E_P$  varies from zero (volume-activated dynamics) to unity (thermally activated dynamics) with increasing dominance of temperature in governing  $\tau_\alpha$ . Using the relation<sup>48,66</sup>

$$E_V/E_P = 1 + \gamma T \alpha_P(T) \quad (3)$$

we calculate  $E_V/E_P = 0.61$  and  $0.74$  respectively for P2CS and PVME neat at  $T_g$ . Such values are typical of polymers, among which the ratio varies from  $0.52$  to  $0.81$ <sup>35</sup> (with the singular exception of poly(phenylene oxide), for which  $E_V/E_P = 0.25$ <sup>63</sup>).

In the blend the scaling exponent for P2CS decreases from  $\gamma = 2.6$  to  $1.9$ , revealing that steric constraints (jamming) are less effective in the blend compared to the neat material. For PVME  $\gamma$  increases from  $2.55$  to  $2.9$ , indicating an enhanced volume effect in the blend. Thus, high-pressure measurements on this blend reveal the contributions of the inherent chemical structure ( $\gamma$  of the neat components) and of the intermolecular cooperativity arising from constraints imposed by the local environment (changes of  $\gamma$  upon blending). Such information cannot be gleaned from experiments on pure components only or from measurements that do not employ pressure as an experimental variable.

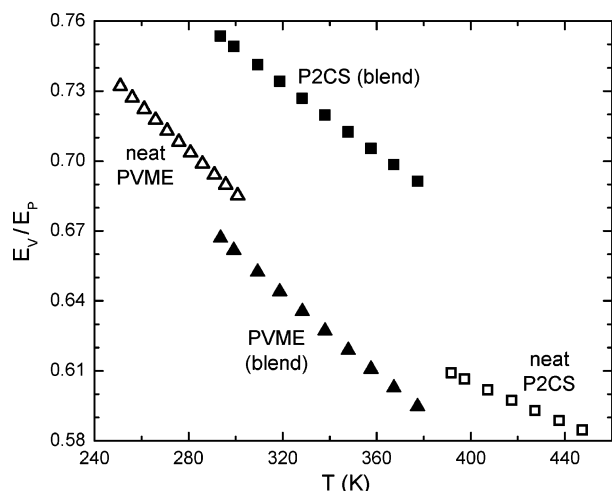


**Figure 10.** Activation enthalpy ratio at  $P = 0.1$  MPa as a function of temperature for the two polymers neat (hollow symbols) and in the blend (solid symbols).

While the scaling exponents in Table 1 are independent of  $T$  and  $P$ , the activation enthalpy ratio, which gives a more direct measure of the relative effect of volume on the dynamics, is not. It is a general trend that as the dynamics are enhanced (e.g., higher temperature or lower pressure), the role of volume on the dynamics increases.<sup>67</sup> This is seen directly (Figure 10) in the change in  $E_v/E_p$  with temperature, calculated for ambient pressure using eq 3. The data, extending from  $T_g$  and above, are for the two components neat and in the blend. For all cases, increasing temperature increases the effect that that volume has on the dynamics compared to that from temperature. The relative positions of the curves parallel effect of blending, as also reflected in the changes in the respective values of the scaling exponents.

Interestingly, the scaling exponent for the ionic conductivity,  $=1.7$ , is smaller than  $\gamma$  for either component (Figure 8). Although the ionic impurities are unidentified, they are smaller than the polymer chain segments. For a small diffusing particle, the chain segments pose barriers that are less sterically restrictive than for segmental motion per se; hence, the motion of the ions is less density dependent than is  $\tau_\alpha$ . Since the relative contribution of energy and volume differs for the two components, however, there is a different degree of translational–rotational decoupling under isobaric conditions (Figure 9b). At fixed temperature (Figure 9a), this is no longer the case.

**Models for Blend Dynamics.** The changes in  $\gamma$  due to blending do not follow from any simple, generalized mixing rule, according to which blend properties are expected to be intermediate between those of the pure component. For example, glass transition temperatures often conform rather well to the Fox equation<sup>68</sup>

$$T_g(\phi_1) = \left( \frac{\phi_1}{T_{g,1}} + \frac{1 - \phi_1}{T_{g,2}} \right)^{-1} \quad (4)$$

in which  $\phi_1$  is the volume fraction of component 1. This expression presumes a single  $T_g$  in miscible blends, thus ignoring dynamic heterogeneity. For the present blend ( $\phi = 0.5$ ), eq 4 predicts  $T_g = 307$  K, which is 18 deg above  $T_g$  of the blend,  $=289.1$  K in Table 1. (Leroy et al.<sup>34</sup> have shown that an empirical equation<sup>69</sup> gives a better fit than eq 4 for this particular blend; however, the expression has two adjustable parameters which must be determined for every blend.) Thus, the dynamics in this blend are faster (lower  $T_g$ ) than expectations based on this simple mixing rule.

A model<sup>2</sup> that explicitly considers dynamic heterogeneity uses a variation of eq 4 to deduce the local  $T_g$ 's associated with subvolumes, whose size according to the model is defined by the Kuhn step length of the chain. The local composition is altered by chain connectivity from the average value  $\phi$  to an effective concentration,  $\phi_{\text{eff}}$ ; thus,  $\phi_{\text{eff}} = \phi_{\text{self}} + (1 - \phi_{\text{self}})\phi$ , where  $\phi_{\text{self}}$  accounts for the excess of segments due to the chain connectivity (i.e., enrichment,  $\phi_{\text{eff}} > \phi$ ). Thus, the modified Fox equation is<sup>2</sup>

$$T_g(\phi_1) = \left( \frac{\phi_{\text{eff}}}{T_{g,1}} + \frac{1 - \phi_{\text{eff}}}{T_{g,2}} \right)^{-1} \quad (5)$$

Rather than calculate  $\phi_{\text{self}}$  from the chain properties, a common practice is to treat it as an adjustable parameter to yield agreement with experimental results.<sup>17,70,71</sup> Using the data in Table 1, eq 5 gives  $\phi_{\text{eff}} = 0.437$  for the P2CS. Since this is less than the actual concentration (i.e.,  $\phi_{\text{self}} < 0$ ), the implication is no enrichment due to the intramolecularly bonded neighboring segments.

This calculation suggesting the absence of self-concentration effects for P2CS in the blend does not negate the idea that the local concentration is enriched due to chain connectivity. However, it does call into question the significance of this enrichment over the length scale associated with segmental relaxation. It should also be recognized that eq 4 is not always quantitatively accurate,<sup>63,72–75</sup> particularly when there is specific interaction between the components. The miscibility between P2CS and PVME arises due to specific interaction between the phenyl ring and the methoxy group,<sup>29,30</sup> which might contribute to the failure of the Fox equation herein. Certainly more measurements extending to other compositions would help resolve this issue.

**Acknowledgment.** This work was supported by the Office of Naval Research.

## References and Notes

- (1) Chung, G. C.; Kornfield, J. A.; Smith, S. D. *Macromolecules* **1994**, *27*, 964.
- (2) Lodge, T. P.; McLeish, T. C. B. *Macromolecules* **2000**, *33*, 5278.
- (3) Miller, J. B.; McGrath, K. J.; Roland, C. M.; Trask, C. A.; Garroway, A. N. *Macromolecules* **1990**, *23*, 4543.
- (4) Colby, R. H. *Polymer* **1989**, *30*, 1275.
- (5) Pathak, J. A.; Colby, R. H.; Floudas, G.; Jerome, R. *Macromolecules* **1999**, *32*, 2553.
- (6) Roland, C. M.; Ngai, K. L. *Macromolecules* **1991**, *24*, 2261.
- (7) Hoffmann, S.; Richter, D.; Arbe, A.; Colmenero, J.; Farago, B. *Appl. Phys. A: Mater. Sci. Process.* **2002**, *74*, S442.
- (8) Alegria, A.; Telleria, I.; Colmenero, J. *J. Non-Cryst. Solids* **1994**, *172*, 961.
- (9) Roland, C. M.; Santangelo, P. G.; Baram, Z.; Runt, J. *Macromolecules* **1994**, *27*, 5382.
- (10) Roland, C. M.; Santangelo, P. G.; Ngai, K. L.; Meier, G. *Macromolecules* **1993**, *26*, 6164.
- (11) Roland, C. M. *Macromolecules* **1995**, *28*, 3463.
- (12) Ngai, K. L.; Roland, C. M. *Rubber Chem. Technol.* **2004**, *77*, 579.
- (13) Roland, C. M.; Ngai, K. L. *Macromolecules* **1992**, *25*, 363; **2000**, *33*, 3184.
- (14) Katana, G.; Fischer, E. W.; Hack, Th.; Abetz, V.; Kremer, F. *Macromolecules* **1995**, *28*, 2714.
- (15) Kumar, S. K.; Colby, R. H.; Anastasiadis, S. H.; Fytas, G. *J. Chem. Phys.* **1996**, *105*, 3777.
- (16) Kamath, S.; Colby, R. H.; Kumar, S. K. *Macromolecules* **2003**, *36*, 8567.
- (17) Haley, J. C.; Lodge, T. P.; He, Y.; Ediger, M. D.; von Meerwall, E. D.; Mijovic, J. *Macromolecules* **2003**, *36*, 6142.
- (18) Leroy, E.; Alegria, A.; Colmenero, J. *Macromolecules* **2003**, *36*, 7280.
- (19) Cangialosi, D.; Schwartz, G. A.; Alegria, A.; Colmenero, J. *J. Chem. Phys.* **2005**, *123*, 144908.
- (20) Lutz, T. R.; He, Y. Y.; Ediger, M. D. *Macromolecules* **2005**, *38*, 9826.
- (21) Sy, J. W.; Mijovic, J. *Macromolecules* **2000**, *33*, 933.

- (22) Jin, X.; Zhang, S. H.; Runt, J. *Macromolecules* **2004**, *37*, 8110.
- (23) Jin, X.; Zhang, S. H.; Runt, J. *Macromolecules* **2004**, *37*, 4808.
- (24) Mpoukouvelas, K.; Floudas, G.; Zhang, S. H.; Runt, J. *Macromolecules* **2005**, *38*, 552.
- (25) Mpoukouvelas, K.; Floudas, G.; Verdonck, B.; Du Prez, F. E. *Phys. Rev. E* **2005**, *72*, 011802.
- (26) Floudas, G.; Fytas, G.; Reisinger, T.; Wegner, G. *J. Chem. Phys.* **1999**, *111*, 9129.
- (27) Milhaupt, J. M.; Lodge, T. P.; Smith, S. D.; Hamersky, M. W. *Macromolecules* **2001**, *34*, 5561.
- (28) Neelakantan, A.; Maranas, J. K. *Macromolecules* **2006**, *39*, 8473.
- (29) Mirau, P. A.; Bovey, F. A. *Macromolecules* **1990**, *23*, 4548.
- (30) Tran-Cong, O.; Nakano, H.; Okinaka, J.; Kwakubo, R. *Polymer* **1994**, *35*, 1242.
- (31) Ngai, K. L.; Roland, C. M. *Macromolecules* **1995**, *28*, 4033.
- (32) Neelakantan, A.; May, A.; Maranas, J. K. *Macromolecules* **2005**, *38*, 6598.
- (33) Urakawa, O.; Fuse, Y.; Hori, H.; Tran-Cong, Q.; Yano, O. *Polymer* **2001**, *42*, 765.
- (34) Leroy, E.; Alegría, A.; Colmenero, J. *Macromolecules* **2002**, *35*, 5587.
- (35) Roland, C. M.; Hensel-Bielowka, S.; Paluch, M.; Casalini, R. *Rep. Prog. Phys.* **2005**, *68*, 1405.
- (36) Alegría, A.; Gómez, D.; Colmenero, J. *Macromolecules* **2002**, *35*, 2030.
- (37) Floudas, G. In *Broadband Dielectric Spectroscopy*; Kremer, F., Schonhals, A., Eds.; Springer-Verlag: Berlin, 2003; Chapter 8.
- (38) Casalini, R.; Roland, C. M. *J. Chem. Phys.* **2003**, *119*, 4052.
- (39) Roland, C. M.; Casalini, R. *J. Chem. Phys.* **2003**, *119*, 1838.
- (40) Cook, R. E.; King, H. E.; Peiffer, D. G. *Phys. Rev. Lett.* **1992**, *69*, 3072.
- (41) Poole, P. H.; Sciortino, F.; Grande, T.; Stanley, H. E.; Angell, C. A. *Phys. Rev. Lett.* **1994**, *73*, 1632.
- (42) Czelik, C.; Jonas, J. *Chem. Phys. Lett.* **1999**, *302*, 633.
- (43) Mammone, J. F.; Sharma, S. K.; Nicol, M. J. *Phys. Chem.* **1980**, *84*, 3130.
- (44) Root, L. J.; Berne, B. J. *J. Chem. Phys.* **1997**, *107*, 4350.
- (45) Arencibia, A.; Taravillo, M.; Pérez, F. J.; Núñez, J.; Baonza, V. G. *Phys. Rev. Lett.* **2002**, *89*, 195504.
- (46) Naoki, M.; Katahira, S. *J. Phys. Chem.* **1995**, *95*, 431.
- (47) Zhang, S. H.; Casalini, R.; Runt, J.; Roland, C. M. *Macromolecules* **2003**, *36*, 9917.
- (48) Casalini, R.; Roland, C. M. *Phys. Rev. E* **2004**, *69*, 062501.
- (49) Dreyfus, C.; Le Grand, A.; Gapinski, J.; Steffen, W.; Patkowski, A. *Eur. Phys. J.* **2004**, *42*, 309.
- (50) Zoller, P.; Walsh, D. J. *Standard Pressure–Volume–Temperature Data for Polymers*; Technomic: Lancaster, PA, 1995.
- (51) Rabeony, M.; Lohse, D. J.; Garner, R. T.; Han, S. J.; Graessley, W. W.; Migler, K. B. *Macromolecules* **1998**, *31*, 6511.
- (52) Schonhals, A.; Kremer, F. Chapter 1 in ref 37.
- (53) Orwoll, R. A. In *Physical Properties of Polymers Handbook*; Mark, J. E., Ed.; American Institute of Physics: Woodbury, NY, 1996; Chapter 7.
- (54) Sasabe, H.; Saito, S. *Polym. J.* **1972**, *3*, 624.
- (55) Fujara, F.; Geil, B.; Sillescu, H.; Fleischer, G. Z. *Phys. B* **1992**, *88*, 195.
- (56) Rossler, E.; Tauchert, J.; Eiermann, P. *J. Phys. Chem.* **1994**, *98*, 8173.
- (57) Cicerone, M.; Blackburn, F. R.; Ediger, M. D. *J. Chem. Phys.* **1995**, *102*, 471.
- (58) Ngai, K. L.; Casalini, R.; Capaccioli, S.; Paluch, M.; Roland, C. M. *J. Phys. Chem. B* **2005**, *109*, 17356.
- (59) Roland, C. M.; Casalini, R.; Paluch, M. *Chem. Phys. Lett.* **2003**, *367*, 259.
- (60) Angell, C. A. *Polymer* **1997**, *38*, 6261.
- (61) Böhmer, R.; Ngai, K. L.; Angell, C. A.; Plazek, D. J. *J. Chem. Phys.* **1993**, *99*, 4201.
- (62) Lorthioir, C.; Alegría, A.; Colmenero, J. *Eur. Phys. J.* **2003**, *12*, 29.
- (63) Roland, C. M.; Casalini, R. *Macromolecules* **2005**, *38*, 8729.
- (64) Hoffman, J. D.; Williams, G.; Passaglia, E. *J. Polym. Sci.* **1966**, *C14*, 173.
- (65) Naoki, M.; Endou, H.; Matsumoto, K. *J. Phys. Chem.* **1987**, *91*, 4169.
- (66) Casalini, R.; Roland, C. M. *Colloid Polym. Sci.* **2004**, *283*, 107.
- (67) Roland, C. M.; McGrath, K. J.; Casalini, R. *J. Non-Cryst. Solids*, in press.
- (68) Fox, T. G. *Bull. Am. Phys. Soc.* **1956**, *1*, 123.
- (69) Brekner, M. J.; Schneider, H. A.; Cantow, H. J. *Polymer* **1988**, *29*, 78.
- (70) He, Y.; Lutz, T. R.; Ediger, M. D. *J. Chem. Phys.* **2003**, *119*, 9956.
- (71) Lutz, T. R.; He, Y.; Ediger, M. D.; Cao, H.; Lin, G.; Jones, A. A. *Macromolecules* **2003**, *36*, 1724.
- (72) Wen, G. Y.; An, L. J. *J. Appl. Polym. Sci.* **2003**, *90*, 959.
- (73) Ishida, H.; Lee, Y. H. *J. Appl. Polym. Sci.* **2001**, *81*, 1021.
- (74) Cantor, A. S. *J. Appl. Polym. Sci.* **2000**, *77*, 826.
- (75) Mohanty, S.; Nando, G. B.; Vijayan, K.; Neelakanthan, N. R. *Polymer* **1996**, *37*, 5387.

MA060315K